Particle size and shape characterization of feedstock material for biofuel production

V. Chaloupková, T. Ivanova[*] and V. Krepl

Czech University of Life Sciences, Faculty of Tropical AgriSciences, Department of Sustainable Technologies, Kamýcká 129, CZ165 00 Prague, Czech Republic
[*]Correspondence: ivanova@ftz.czu.cz

Abstract. Particle size and shape are key factors influencing the properties of particulate and agglomerated materials, and having an impact on a quality as well as utilization of a final product. In case of plant biomass particle morphology is greatly irregular. Large errors at most determinations of biomass particle sizes are caused by simplification on a single parameter of size, assuming particle sphericity or circularity. Thus, the aim of a present research was to determine the particle size in a complex way. Pine sawdust as an experimental material and typical biofuel feedstock was ground by a hammer mill to a fraction size of 12 mm. The dimensional features of such ground sawdust particles were identified for all particles individually via photo-optical analysis, a method based on a digital image processing that is sensitive to irregular particles' shapes. The particles were described mainly by variables of length, max width, equivalent diameter, max and min feret diameter, sphericity, roundness, circularity together with length/width ratio and aspect ratio. Data were analysed by descriptive statistics, i.e. by arithmetic means, medians, minimum and maximum values, variance and standard deviation. The obtained results may contribute to a better knowledge of material properties needed for designing an optimal technology for the production of quality biofuels.

Key words: particle morphology, size variable, pine sawdust, photo-optical analysis.

INTRODUCTION

Understanding of particle morphological and rheological behaviour as well as measuring particle size and comprehension how it affects processes and final products can be critical to the success of many manufacturing businesses and industries (Shekunov et al., 2006; Guo et al. 2012; Vaezi et al., 2013; Agimelen et al., 2017; Cardona et al., 2018). In case of biomass it is significant in fields associated with the particle handling, transportation, mixing, dosing, flow-ability, densification, fluidization, gasification or combustion (Gil et al., 2014; Ahmad et al., 2016; Holmgren et al., 2017; Trubetskaya et al., 2017; Knoll et al., 2019).

Particle size and shape measurement has long tradition in soil and sediment sciences (Cox, 1927; Wadell, 1932; Krumbein, 1941; Koerner, 1970) and core of biomass morphology characterization originates from these disciplines. Classification of particular material based on dimensional properties has long been based upon sieve analysis where the material is separated by sieves of differently sized apertures into fractions of particle size distribution (Fernlund, 1998). This traditional approach

considers only one parameter: general particle diameter which is given by the aperture of a sieve (Igathinathane et al., 2009a). Often, particle morphology is simplified by a single parameter size, assuming sphericity or circularity (Lu et al., 2010; Ulusoy & Igathinathane, 2016). This assumption is convenient owing to numerous findings about behaviour properties of spherical particles (Walpole, 1972; Riguidel et al., 1994; Niazmand & Renksizbulut, 2003; Antonyuk et al., 2005). However presuming sphericity in case of biomass particle modelling is inadequate (Trubetskaya et al., 2017) and may result in large errors at most particle size estimations (Lu et al., 2010).

Due to high and varied proportion of cellulose, hemicellulose and lignin in biomass composition which is different for all plant species, the morphology of grinded/milled biomass is greatly non-uniform (Guo et al., 2012; Febbi et al., 2015). Biomass particles are in practise non-spherical and irregular (Dai et al., 2012). Since the particle size and shape are complex parameters (Fernlund, 1998), at least two parameters are necessary to describe particle size/shape (Trubetskaya et al., 2017). It can be represented by several variables, such as length, width, diameter, perimeter, surface area, volume and descriptors calculated from them, like sphericity, roundness and ratios of two object dimensions (Murphy, 1984; Vaezi et al., 2013; Bagheri et al., 2015; Zhao & Wang, 2016). There are several shapes qualitatively described by various studies, for instance flakes, rod-like and needle-like particle (Guo et al., 2012), or plate, slab, prism, cylinder, rod and sphere (Liliedahl & Sjoèstroèm, 1998; Saastamoinen, 2006). Despite numerous studies on biomass particle morphology, there is no universal consensus on how to represent a biomass particle size and shape in some details, thus the combination of several descriptors is needed (Pons et al., 1999).

Computer vision-based methods are getting growing interest in various fields where greater precision, efficiency, quality and performance of observed objects are highly demanded (Davies, 2018). This approach can be used for two (2D) or three (3D) dimensional image analysis of particle morphology and particle size distribution (Zhao & Wang, 2016; Sunoj et al., 2018), where it is interesting alternative or even substitution for the traditional sieve analysis (Igathinathane et al., 2009a; Igathinathane et al., 2009b; Souza & Menegalli, 2011; Kumara et al., 2012; Gil et al., 2014; Febbi et al., 2015; Chaloupková et al., 2018). The image analysis is the technique being sensitive to the particle geometrical shape and considering more parameters than just sphericity which leads to more precise results (Dai et al., 2012; Ulusoy & Igathinathane, 2016).

More accurate data about material properties together with process variables may enhance efficiency of biomass energy conversion processes and may bring optimal products of higher quality with desired properties (Ndindeng et al., 2015). Thus, the aim of the present research was to determine the particle size and shape of pine sawdust in a complex way using a photo-optical analyser and 2D imaging.

MATERIALS AND METHODS

Pine sawdust (*Pinus* spp.) as a typical feedstock material for solid biofuel production (Deac et al., 2016) was selected as the experimental material in this study. The material originated from the Czech Republic was grinded into the fraction size of 12 mm by the hammer mill (model 9FQ - 40C, Pest Control Corporation, Ltd., Vlčnov, Czech Republic). Such prepared material was dried to the moisture content (w.b.) of

8.39% (determined according to EN ISO 18134-2, 2017) to decrease particle adhesion and agglomeration during the measurement.

A computerized photo-optical particle analyser Haver (model CPA 4-2, Haver & Boecker OHG, Oelde, Germany) was used to analyse particle properties. The automatic analyser worked under the particle measuring range 0.091–90 mm which was selected with respect to the material character. The analyser consisted of a feeding unit with the high of 6 mm being set for the regular and even particle layout on a vibration channel, a vibratory channel itself, an optical sensor in the form of CCD-line digital scan camera with the high-resolution (4,096 pixels line resolution) that scanned all free-falling particles of the studied sample against the background of a red LED lighting array module with a high recording frequency (up to 28,000 line scans per second) (Haver & Boecker, 2015). Amplitude of the vibrating feeder (feed rate) was automatically regulated by the analyzer as the particles were falling down. Minimum and maximum values of optical density were set as 0.5 and 2, respectively. Shape model was set as '*elongated*' and volume model as '*elliptical segment*'. Control of the entire measurement process and data evaluation were performed from a portable computer equipped with a Gigabit Ethernet (GigE) interface as well as a RS 232 interface that was connected to the analyser. All passed particles were individually recorded, measured and their 2D profile parameters were processed via Haver CpaServ software (Haver & Boecker OHG, Oelde, Germany). The scanned particles were analysed in terms of variables stated and defined in the Table 1.

Obtained data were processed using MS Excel (version 2007, Microsoft, Redmond, WA, USA) and Statistica software (version 13.3, TIBCO Software Inc., Palo Alto, CA, USA) and summarized by descriptive statistics, i.e. measures of central tendencies (means), measures of variability and frequency distributions. Afterwards the obtained results were tabulated, graphically plotted and discussed.

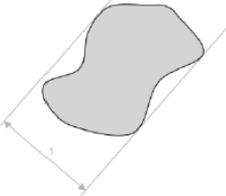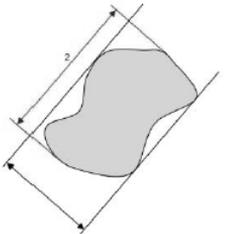**Table 1.** Variables measured by the photo-optical analyser

| Variable and definition	Diagram
Minimum feret diameter (X_{min}) Minimum distance of two tangents, which can be placed in parallel onto the outer particle contour (Haver & Boecker, 2014)	
Length (L) The length is determined perpendicularly to the minimum feret diameter and it corresponds to the long side of a rectangular shaped projection area; used for calculation of length/width ratio (R_{lw}) (Haver & Boecker, 2014)	
Maximum feret diameter (X_{max}) Maximum distance between two parallel tangents of the particle contour (Haver & Boecker, 2014)	

Table 1 (continued)

Maximum width (W_{max})
Maximum extension of the particle projection area
orthogonally to the maximum length
(Haver & Boecker, 2014)
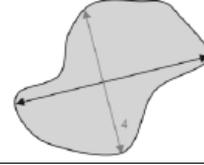
Equivalent diameter (X_a)
Diameter of a circle, the surface area of which corresponds to the projected area of the particle
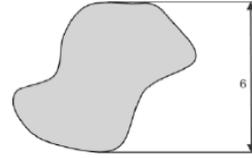(Olson, 2011)

$$X_a = \sqrt{\frac{4 * A_1}{\pi}} \qquad (1)$$
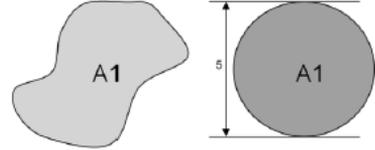
Projection area (A_1)
Sum of the areas of individual pixel (Olson, 2011)

$$A_1 = \sum a_p \qquad (2)$$

where a_p is area of each individual pixel

Feret diameter* (X)
Distance between two parallel tangents of the particle
contour, vertical to the direction of measurement
(Haver & Boecker, 2014)

Martin-diameter* (X_m)
Length from the particle projection, it is the line that cuts
the area in half, horizontally to the direction of
measurement (Haver & Boecker, 2014)
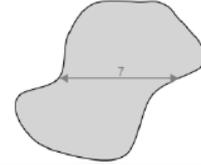
Circularity (C)
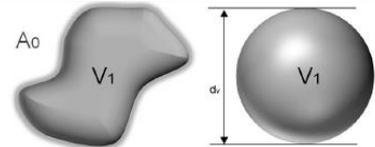Degree of similarity of the particle projection area with a circle (Haver & Boecker, 2014)

$$C = \frac{U_p}{(2 * \sqrt{\pi * A_1})} \qquad (3)$$

Where U_p is measured perimeter of particle and A_1
measured projected area
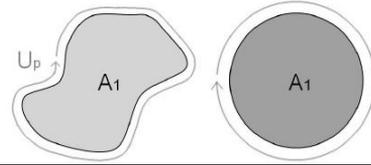
Sphericity (ψ)
Degree of similarity of the particle with a sphere

$$\psi = \frac{\pi \cdot d_v}{A_0} \qquad (4)$$

where A_0 is the particle's calculated surface area and d_v is the diameter of an equal volume sphere
(Wadell, 1932)

Roundness (R_d)
Degree of roundness the particle corners and edges (Wadell, 1932)

$$R_d = \frac{\frac{1}{n}\sum_{i=1}^{n} r_i}{r_{max}} \qquad (5)$$

where r_i is the radius of the i-th corner curvature, n the number of corners, and r_{max} the radius of
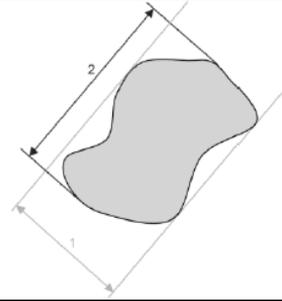the maximum inscribed circle

Table 1 (continued)

Length/width ratio (R_{lw})
The ratio of length to width was calculated from the ratio of length to the minimum feret diameter of the projection area (Haver & Boecker, 2014)

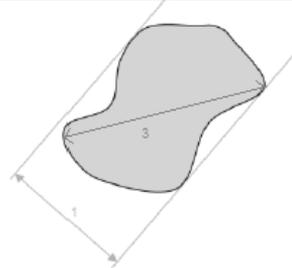$$R_{lw} = \frac{L}{X_{min}} \qquad (6)$$

where L is length and X_{min} minimum feret diameter

Aspect ratio (A_r)
Ratio of maximum (X_{max}) to minimum (X_{min}) feret diameter (Agimelen et al., 2017)
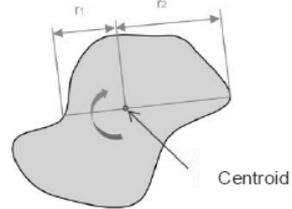
$$A_r = \frac{X_{max}}{X_{min}} \qquad (7)$$

Symmetry (S_m)
For symmetry, the area centroid of the particle is determined.

Axes of symmetry run through the centroid. These axes are rotated in 1° increments. Here the ratio of radii is computed. The smallest result is denoted as the symmetry (Haver & Boecker, 2014)

$$S_m = \frac{r_1}{r_2} \qquad (8)$$

where r_1 is the smallest radius and r_2 the largest radius

Perimeter (U_p)
Total length of the particle boundary (Olson, 2011)

$$U_p = \frac{\pi}{N} \sum_{\alpha}^{\pi} I_\alpha \, d_L \qquad (9)$$

Where I is number of intercepts, formed by series of parallel lines, with spacing dL, exploring N directions, from α to π
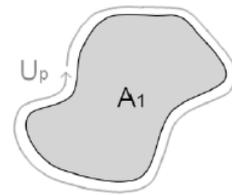
Notes: * position-dependent size; All diagrams adopted from Haver & Boecker (2014).

RESULTS AND DISCUSSION

In total 536,137 pine sawdust particles were analysed by the photo-optical image analyser to identify the particle morphology. This number brings precise statistical data, as Masuda & Gotoh (1999) determined that about 61,000 particles are required in order to get the mass median diameter within 5% error with 95% probability for a powder having a geometric standard deviation of 1.6.

Fig. 1 shows the 2D projections of selected pine sawdust particles recorded by the analyzer. As it can be seen, the material is composed of un-evenly shaped particles.

Figure 1. 2D projections of selected particles of pine sawdust.

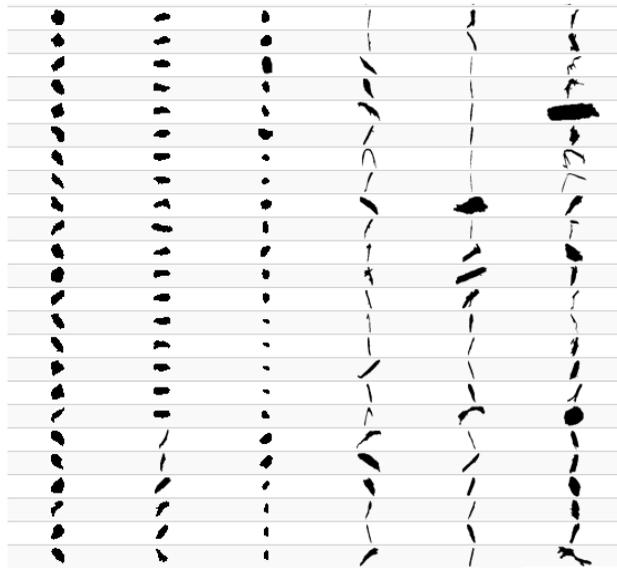Table 2 provides detailed descriptive statistics of the particles' measured variables, i.e. total number of analysed particles, their arithmetic mean, median, mode, frequency of mode, maximum and minimum values, lower and upper quartiles, together with variance, standard deviation and coefficient of variance, rounded to four decimal places.

Diameter of irregular particles is mostly evaluated by X, the distance between two furthest points of the particle is measured in a given direction (Igathinathane et al., 2009a; Dražić et al., 2016). In case of the studied material, mean value of X was 1.12 ± 0.88 mm. More useful information is given by X_{max} and X_{min}, since they calculate a diameter of the particle in all directions (Dražić et al., 2016). X_{max} is often associated to the '*length*' of the particle (Pons et al., 1999). Length of the pine sawdust particles ranged from its maximum of 28.26 mm to its minimum of 0.16 mm (which was given by the measuring possibility of the analyser) and with arithmetic mean of 1.26 ± 0.94 mm. On the contrary, X_{min} is related to the particle '*breadth*' (Pons et al., 1999). Mean, min and max values of X_{min} were 0.51 ± 0.33 mm, 0.09 mm and 10.04 mm, respectively. Feret diameter as an algorithm for particle dimension is often used to evaluate particle size distribution (Igathinathane et al., 2009a). X_{max} gives the value of the minimum sieve size through which the particle can pass through without any obstacle (Shanthi et al., 2014). On the Fig. 2 there is illustrated the histogram of X_{max}, where the particles are grouped into the fractions based on the sizes (holes' diameters) of standard sieves (EN ISO 17827-1, 2, 2016).

The observation indicates the increased presence of fine particles, since most of the material (~71%) has size of 1.0–2.0 mm. Even though the material was grinded into fraction size of 12 mm, only ~5% of the material has $X_{max} > 2.8$ mm. Presented result should be theoretically obtained by traditional oscillating analysis.

Table 2. Descriptive statistics of measured variables

Variable	Mean	Median	Mode	Mode Freq.	Min	Max	Lower Quart.	Upper Quart.	Var.	Std. Dev.	Coef. Var.
Min feret X_{min}[a]	0.5105	0.4550	0.0910	47,696	0.0910	10.0377	0.2730	0.6402	0.1078	0.3283	64.3059
Length L[a]	1.2292	1.0163	0.6083	21,668	0.0910	28.2639	0.6954	1.4877	0.8964	0.9468	77.0283
Max feret X_{max}[a]	1.2635	1.0596	0.1257	10,903	0.1257	28.2639	0.7188	1.5219	0.8859	0.9412	74.4932
Max width W_{max}[a]	0.4995	0.4569	0.1206	10,903	0.0869	8.7320	0.2826	0.6438	0.1016	0.3188	63.8187
Equiv.diam. X_a[a]	0.6591	0.6024	0.1003	10,903	0.1003	7.6619	0.4199	0.8222	0.1374	0.3707	56.2369
Feret X[a]	1.1179	0.8697	0.6083	40,002	0.0868	28.2639	0.6083	1.3064	0.7797	0.8830	78.9922
Martin diam. X_m[a]	0.5233	0.4550	0.3640	70,052	0.0910	12.1940	0.2730	0.6370	0.1569	0.3961	75.6862
Circularity C[d]	0.7280	0.7549	0.8860	10,903	0.1231	0.9732	0.6425	0.8367	0.0192	0.1385	19.0210
Sphericity ψ[d]	0.7008	0.7198	0.2964	10,903	0.2381	0.8735	0.6684	0.7579	0.0092	0.0957	13.6518
Roundness R_d[d]	0.3456	0.3429	0.6359	10,903	0.0064	0.8089	0.2330	0.4539	0.0219	0.1479	42.7937
Length/width R_{lw}[d]	3.0372	2.2223	1.0424	10,903	1.0128	90.6745	1.6299	3.3538	7.0271	2.6509	87.2802
Aspect ratio A_r[d]	2.9255	2.1544	1.3816	10,903	1.0687	55.0247	1.6328	3.2416	5.7653	2.4011	82.0755
Symmetry S_m[d]	0.6247	0.6393	1.0000	40,652	0.0000	1.0000	0.5181	0.7331	0.0423	0.2057	32.9203
Perimeter U_p[a]	3.0789	2.5701	0.3555	10,903	0.3555	78.2456	1.7621	3.7086	5.5166	2.3487	76.2843
Proj. Area A_l[b]	0.4491	0.2850	0.0079	10,903	0.0079	46.1066	0.1385	0.5309	0.4667	0.6832	152.1229
Surface area A_0[b]	2.0446	1.2985	0.0248	10,903	0.0248	226.9127	0.6343	2.4250	10.0162	3.1648	154.7911
Volume V_l[c]	0.2394	0.0825	0.0001	10,903	0.0001	127.0393	0.0277	0.2104	0.9265	0.9626	402.1449

Total count of observations: 536,137.

Notes: [a] in [mm]; [b] in [mm^2]; [c] in [mm^3]; [d] calculated as the ratio, i.e. without unit.

L, W_{max}, X_m and X_a define particle size in different manners (Pons et al., 1999). Mean value for L was 1.23 ± 0.95 mm, W_{max} 0.50 ± 0.32 mm, (X_m) 0.52 ± 0.40 mm and X_a 0.66 ± 0.37 mm. Mean X_m is smaller than X_a and both descriptors have smaller mean values than mean X; this corresponds with experimental evidence of other studies (Yang, 2003).
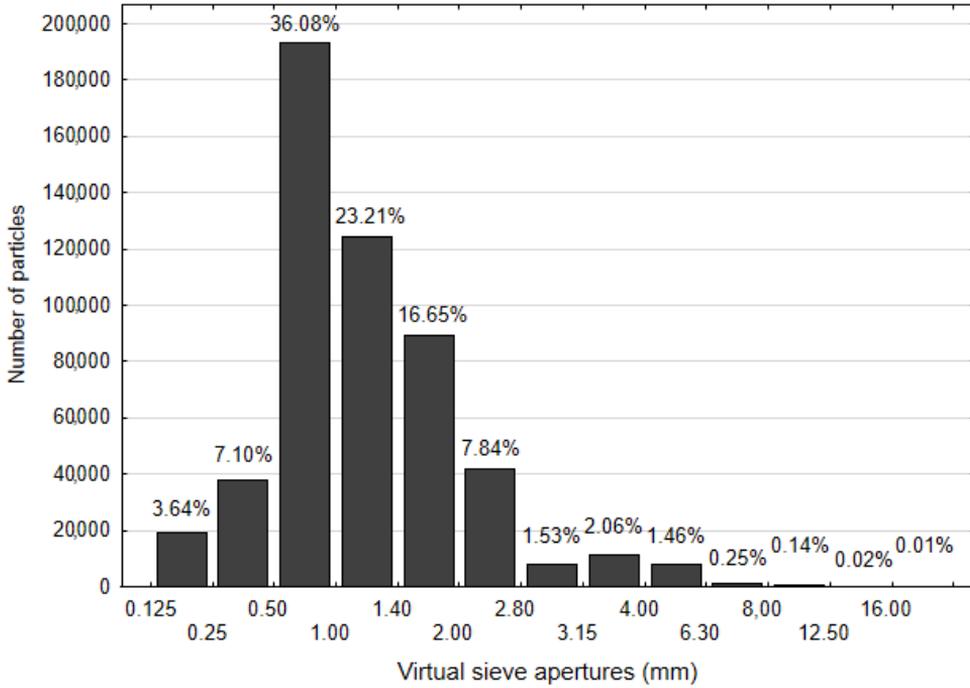

Figure 2. PSD of measured pine sawdust with max feret diameter (X_{max}) as measuring algorithm (in mm).

Shape of particles was defined by C, ψ and R_d, important parameters describing particle shape in several studies (Mora & Kwan, 2000; Cruz-Matías et al., 2019). They were measured in the range of 0.01–1. ψ describes a compactness of a particle in terms of the surface area (Zhao & Wang, 2016) and it is the most dependent on elongation (Olson, 2011; Cruz-Matías et al., 2019). R_d is a characteristic affected by a form, it is not a degree of ψ (ψ is a measure of a form) even though R_d is the best manifested by a perfect sphere. R_d is mainly dependent on the sharpness/roughness of angular convexities and concavities of a particle (Cruz-Matías et al., 2019). R_d of the corners is the opposite of the angularity of the corners and plays significant role in the abrasive and perforation features of the particles (Mora & Kwan, 2000). Wadell (1932) identified ψ and R_d as two independent aspects of a particle shape, however lately Zhao & Wang (2016) reported their dependency. In general, the particles that have larger ψ values also have larger values of A_r and mean R_d value (Zhao & Wang, 2016).

The sphericity index value of a perfect sphere is 1. In case of studied pine sawdust the ψ mean value was 0.70 ± 0.09, thus the particles can be described as irregular (non-spherical) since their average ψ value is smaller than 0.8 (Zhao & Wang, 2016). Fig. 3 shows frequency distributions of ψ together with R_d. For an absolutely round and smooth object (i.e. sphere) the value of R_d is 1, for any other object the values is less than 1. According to the classification of Powers (1953), approx. 1% of particles, as it can be seen from the Fig. 3, is well rounded (range 0.70–1.0) and 18% rounded (range 0.49–0.70). The measured particles can be classified as subangular and subrounded since the average R_d is 0.35 ± 0.15 and majority (~53%) of the material belongs to the range of 0.25–0.35 (subangular) and 0.35–0.49 (subrounded). More or less 15% of particles can be called angular and ~14% very angular.
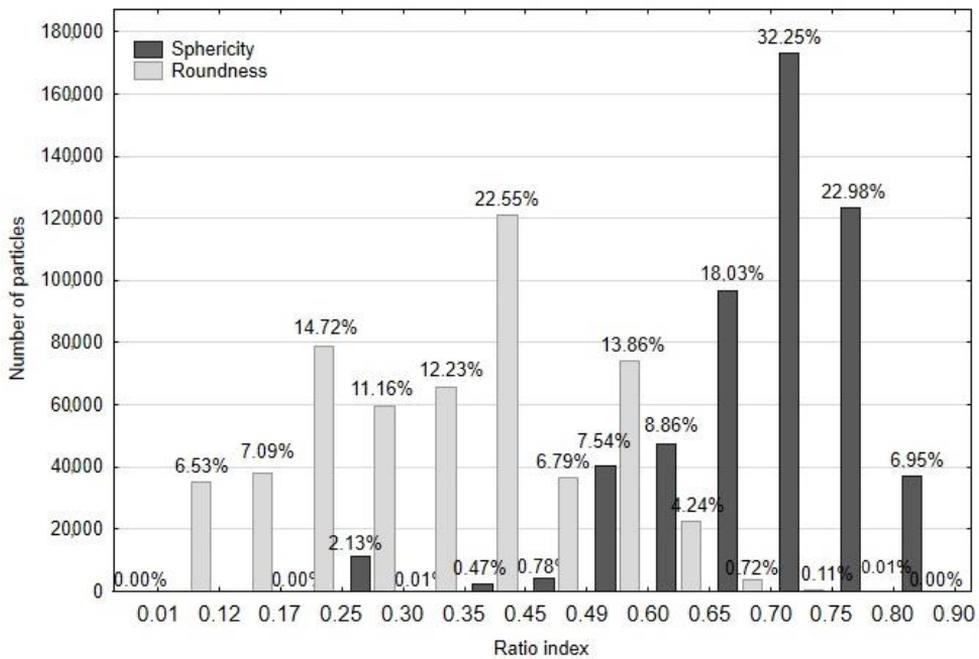

Figure 3. Histograms of sphericity (ψ) and roundness (Rd).

C is a measurement of both the particle form and roughness (Olson, 2011). It can also reach values ranging from 1, as it is in case of particle perfectly round and smooth circle, and up to 0, when conversely shape becomes more angular and rough (Olson, 2011). Average C value of analysed pine sawdust was 0.73 ± 0.14, which means that the particles have slight surface irregularities.

Particle shape can be evaluated also in terms of S_m, ranging from 0 to 1. Perfectly symmetric objects (like sphere or cube) have S_m equal to 1. In case of measured pine sawdust particles mean S_m was 0.62 ± 0.21, so the particles can be called moderately asymmetrical (Yang, 2003).

R_{lw} and A_r show the degree of particle elongation (Agimelen et al., 2017) based on two particle dimensions (Olson, 2011). The ratios can reach values in range of 1–10,000 (Haver & Boecker, 2014). Value 1 is for object with symmetric shape (e.g. sphere or

square) and 10,000 theoretically for very elongated and thin objects, however the ratios are suitable only for particles that are not very elongated and curved (ISO 9276-6, 2008), for example particles of needle-like and acicular shape (Olson, 2011), as it was in case of examined material. Since biomass particles are in practise non-spherical and irregular (Dai et al., 2012), their ratios normally belong to the range 2–15 (Lu et al., 2010). As it can be seen from the Table 2, the measured pine sawdust particles have average value of R_{lw} 3.04 ± 2.65 and A_r 2.93 ± 2.40. Guo et al. (2012) reported similar result for R_{lw} (3.01) of pine milled into 300–425 µm. From the Table 3 it is clear that more than 90% of the material is in the range 1–6 which means that the particles are moderately elongated.

Table 3. Frequency of length/width ratio and aspect ratio values (1–15)

Interval (From – To)	Length/Width ratio R_{lw}			Aspect ratio A_r		
	Count	%	Cumulative %	Count	%	Cumulative %
1 < = x < 1.5	97,935	18.3	18.3	92,320	17.2	17.2
1.5 < = x < 2	132,528	24.7	43.0	136,130	25.4	42.6
2 < = x < 2.5	82,803	15.4	58.4	94,986	17.7	60.3
2.5 < = x < 3	59,140	11.0	69.5	53,578	10.0	70.3
3 < = x < 3.5	34,249	6.4	75.8	42,795	8.0	78.3
3.5 < = x < 4	29,928	5.6	81.4	28,373	5.3	83.6
4 < = x < 4.5	18,756	3.5	84.9	15,526	2.9	86.5
4.5 < = x < 5	15,499	2.9	87.8	15,971	3.0	89.5
5 < = x < 5.5	10,211	1.9	89.7	8,824	1.6	91.1
5.5 < = x < 6	10,017	1.9	91.6	9,581	1.8	92.9
6 < = x < 8	21,525	4.1	95.6	18,703	3.4	96.4
8 < = x < 10	9,992	1.9	97.5	8,629	1.7	98.0
10 < = x < 15	9,818	1.8	99.3	5,151	1.0	99.5

Additional information about the particle morphology gave U_p, A_1, A_0 and V_1. Mean values (together with maximum and minimum values) of these descriptors were U_p 3.08 ± 2.35 mm (0.36–78.25 mm), A_1 0.45 ± 0.68 mm^2 (0.01–46.11 mm^2), A_0 2.04 ± 3.16 mm^2 (0.02–226.91 mm^2) and V_1 0.24 ± 0.96 mm^3 (0.00–127.04 mm^3). Despite of the fact that surface area, volume and sphericity, representing 3D parameters (Zhao & Wang, 2016), were in this study calculated from 2D images, they offered valuable statistical data. 3D imaging could bring more presice results, however this would associated with additional costs of equipment, longer analysing time and smaller amount of analysed particles bringing lower statistical confidence (Bagheri et al., 2015).

CONCLUSIONS

Particle size and shape are important factors that influence the final product's quality. A measurement of a single dimension may not be adequate to describe a typical non-spherical and irregular biomass particle with some extent of surface roughness. In this study particle size and shape of pine sawdust, the typical feedstock material for solid biofuel production, grinded to fraction size of 12 mm, was identified using the photo-optical analyzer based on digital image processing. The photo-optical particle analysis

provided far more detailed information about individual particle physical dimensions than conventional sieving approach, which only yields the cumulative mass curve and overall particle sizes given by the sieve size aperture. From the particle analysis, length, width, max feret, min feret, feret diameter, martin diameter and perimeter were obtained as well as sphericity, roundness, circularity, symmetry, volume, projection area, surface area, together with length/width and aspect ratio were calculated. Particles of pine sawdust can be described as irregular, slightly elongated with moderate degree of angularity, roughness and asymmetry. The real size of particles was much smaller than grinding size, and the fine particles were predominated. The obtained results may contribute to a better knowledge of material properties and facilitate the design of optimal technologies for biomass particle handling and production of quality biofuels with desired properties.

REFERENCES

Agimelen, O.S., Mulholland, A.J. & Sefcik, J. 2017. Modelling of artefacts in estimations of particle size of needle-like particles from laser diffraction measurements. *Chemical Engineering Science* **158**, 445–452.

Ahmad, A.A., Zawawi, N.A., Kasim, F.H., Inayat, A. & Khasri, A. 2016. Assessing the gasification performance of biomass: A review on biomass gasification process conditions, optimization and economic evaluation. *Renewable and Sustainable Energy Reviews* **53**, 1333–1347.

Antonyuk, S., Jürgen, T., Heinrich, S. & Mörl, L. 2005. Breakage behaviour of spherical granulates by compression. *Chemical Engineering Science* **60**(14), 4031–4044.

Bagheri, G.H., Bonadonna, C., Manzella, I. & Vonlanthen, P. 2015. On the characterization of size and shape of irregular particles. *Powder Technology* **270**, 141–153.

Cardona, J., Ferreira, C., McGinty, J., Hamilton, A., Agimelen, O.S., Cleary, A., Atkinson, R., Michie, C., Marshall, S., Chen, Y.-C., Sefcik, J., Andonovic, I. & Tachtatzis, C. 2018. Image analysis framework with focus evaluation for in situ characterisation of particle size and shape attributes. *Chemical Engineering Science* **191**, 208–231.

Cox, E.P.A. 1927. Method of Assigning Numerical and Percentage Values to the Degree of Roundness of Sand Grains. *Journal of Paleontology* **1**(3), 179–183.

Cruz-Matías, I., Ayala, D., Hiller, D., Gutsch, S., Zacharias, M., Estradé, S. & Peiró, F. 2019. Sphericity and roundness computation for particles using the extreme vertices model. *Journal of Computational Science* **30**, 28–40.

Dai, J., Cui, H. & Grace, J.R. 2012. Biomass feeding for thermochemical reactors. *Progress in Energy and Combustion Science* **38**(5), 716–736.

Davies, E.R. 2018. Chapter 1 - Vision, the challenge. In Davies, E. R. (ed.): *Computer Vision (Fifth Edition)*. Academic Press, pp 1–15.

Deac, T., Fechete-Tutunaru, L. & Gaspar, F. 2016. Environmental Impact of Sawdust Briquettes Use – Experimental Approach. *Energy Procedia* **85**, 178–183.

Dražić, S., Sladoje, N. & Lindblad, J. 2016. Estimation of Feret's diameter from pixel coverage representation of a shape. *Pattern Recognition Letters* **80**, 37–45.

EN ISO 17827-1. 2016. Solid biofuels. Determination of particle size distribution for uncompressed fuels. Oscillating screen method using sieves with apertures of 3.15 mm and above. International Organization for Standardization, Geneva.

EN ISO 17827-2. 2016. Solid biofuels. Determination of particle size distribution for uncompressed fuels. Oscillating screen method using sieves with apertures of 3.15 mm and below. International Organization for Standardization, Geneva.

EN ISO 18134-2. 2017. Solid biofuels - Determination of moisture content - Oven dry method - Part 2: Total moisture - Simplified method. International Organization for Standardization, Geneva.

EN ISO 9276-6. 2008. Representation of results of particle size analysis - Part 6: Descriptive and quantitative representation of particle shape and morphology. International Organization for Standardization, Geneva.

Febbi, P., Menesatti, P., Costa, C., Pari, L. & Cecchini, M. 2015. Automated determination of poplar chip size distribution based on combined image and multivariate analyses. *Biomass and Bioenergy* **73**, 1–10.

Fernlund, J.M.R. 1998. The effect of particle form on sieve analysis: a test by image analysis. *Engineering Geology* **50**, 111–124.

Gil, M., Teruel, E. & Arauzo, I. 2014. Analysis of standard sieving method for milled biomass through image processing. Effects of particle shape and size for poplar and corn stover. *Fuel* **116**, 328–340.

Guo, Q., Xueli, C. & Haifeng, L. 2012. Experimental research on shape and size distribution of biomass particle. *Fuel* **94**, 551–555.

Haver & Boecker. 2014. Haver CpaServ Professional/Expert. Manual, Haver & Boecker, 85 pp.

Haver & Boecker. 2015. Haver CPA 4-2, Haver CPA 4 Conveyor, operating instructions. Computer-supported photo-optical particle analysis. Manual, Haver & Boecker, 17 pp.

Holmgren, P., Wagner, D.R., Strandberg, A., Molinder, R., Wiinikka, H., Umeki, K., Broström, M. 2017. Size, shape, and density changes of biomass particles during rapid devolatilization. *Fuel* **206**, 342–351.

Igathinathane, C., Melin, S., Sokhansanj, S., Bi, X., Lim, C.J., Pordesimo, L.O. & Columbus, E.P. 2009a. Machine vision based particle size and size distribution determination of airborne dust particles of wood and bark pellets. *Powder Technology* **196**, 202–212.

Igathinathane, C., Pordesimo, L.O., Columbus, E.P., Batchelor, W.D. & Sokhansanj, S. 2009b. Sieveless particle size distribution analysis of particulate materials through computer vision. *Computers and Electronics in Agriculture* **66**, 147–158.

Knoll, M., Gerhardter, H., Prieler, R., Mühlböck, M., Tomazic, P. & Hochenauer, C. 2019. Particle classification and drag coefficients of irregularly-shaped combustion residues with various size and shape. *Powder Technology* **345**, 405–414.

Koerner, R.M. 1970. Effect of particle characteristics on soil strength. *Journal of the Soil Mechanics and Foundations Division* **96**(4), 1221–1233.

Krumbein, W.C. 1941. Measurement and geological significance of shape and roundness of sedimentary particles. *Journal of Sedimentation Research* **11**(2), 64–72.

Kumara, G., Hayano, K. & Ogiwara, K. 2012. Image analysis techniques on evaluation of particle size distribution of gravel. *International Journal of GEOMATE* **3**(1), 290–297.

Liliedahl, T. & Sjöström, K. 1998. Heat transfer controlled pyrolysis kinetics of a biomass slab, rod or sphere. *Biomass and Bioenergy* **15**(6), 503–509.

Lu, H., Ip, E., Scott, J., Foster, P., Vickers, M. & Baxter, L.L. 2010. Effects of particle shape and size on devolatilization of biomass particle. *Fuel* **89**(5), 1156–1168.

Masuda, H. & Gotoh, K. 1999. Study on the sample size required for the estimation of mean particle diameter. *Advanced Powder Technology* **10**(2), 159–173.

Mora, C.F. & Kwan, A.K.H. 2000. Sphericity, shape factor, and convexity measurement of coarse aggregate for concrete using digital image processing. *Cement and Concrete Research* **30**(3), 351–358.

Murphy, C.H. 1984. *Handbook of particle sampling and analysis methods*. Verlag Chemie International, 354 pp.

Ndindeng, S.A., Mbassi, J.E.G., Mbacham, W.F., Manful, J., Graham-Acquaah, S., Moreira, J., Dossou, J. & Futakuchi, K. 2015. Quality optimization in briquettes made from rice milling by-products. *Energy for Sustainable Development* **29**, (Supplement C), 24–31.

Niazmand, H. & Renksizbulut, M. 2003. Surface effects on transient three-dimensional flows around rotating spheres at moderate Reynolds numbers. *Computers and Fluids* **32**(10), 1405–1433.

Olson, E. 2011. Particle shape factors and their use in image analysis – part 1: Theory. *Journal of GXP Compliance* **15**(3), 85–96.

Pons, M.N., Vivier, H., Belaroui, K., Bernard-Michel, B., Cordier, F., Oulhana, D., Dodds, J.A. 1999. Particle morphology: from visualisation to measurement. *Powder Technology* **103**, 44–57.

Powers, M.C. 1953. A new roundness scale for sedimentary particles. *Journal of Sedimentary Research* 117–119.

Riguidel, F.-X., Jullien, R., Ristow, G.H., Hansen, A. & Bideau, D. 1994. Behaviour of a sphere on a rough inclined plane. *Journal de Physique I France* **4**, 261–272.

Saastamoinen, J.J. 2006. Simplified model for calculation of devolatilization in fluidized beds. *Fuel* **85**(17), 2388–2395.

Shanthi, C., Kingsley Porpatham, R. & Pappa, N. 2014. Image Analysis for Particle Size Distribution. *International Journal of Engineering and Technology* **6**, 5.

Shekunov, B.Y., Chattopadhyay, P., Tong, H.H.Y. & Chow, A.H.L. 2006. Particle Size Analysis in Pharmaceutics: Principles, Methods and Applications. *Pharmaceutical Research* **24**(2), 203–227.

Souza, D.O.C. & Menegalli, F.C. 2011. Image analysis: Statistical study of particle size distribution and shape characterization. *Powder Technology* **214**(1), 57–63.

Sunoj, S., Igathinathane, C. & Jenicka, S. 2018. Cashews whole and splits classification using a novel machine vision approach. *Postharvest Biology and Technology* **138**, 19–30.

Trubetskaya, A., Beckmann, G., Wadenbäck, J., Holm, J.K., Velaga, S.P. & Weber, R. 2017. One way of representing the size and shape of biomass particles in combustion modeling. *Fuel* **206**, 675–683.

Ulusoy, U. & Igathinathane, C. 2016. Particle size distribution modeling of milled coals by dynamic image analysis and mechanical sieving. *Fuel Processing Technology* **143**, 100–109.

Vaezi, M., Pandey, V., Kumar, A. & Bhattacharyya, S. 2013. Lignocellulosic biomass particle shape and size distribution analysis using digital image processing for pipeline hydro-transportation. *Biosystems Engineering* **114**(2), 97–112.

Wadell, H.A. 1932. Volume, Shape and Roundness of Rock Particles. *The Journal of Geology* **40**, 443–451.

Walpole, L.J. 1972. The elastic behaviour of a suspension of spherical particles. *The Quarterly Journal of Mechanics and Applied Mathematics* **25**(2), 153–160.

Yang, W.-C. 2003. Flow through fixed beds. In Yang, W.-C. (ed.): *Handbook of fluidization and fluid-particle systems.* Marcel Dekker, Inc: New York, pp. 29–53.

Zhao, B. & Wang, J. 2016. 3D quantitative shape analysis on form, roundness, and compactness with μCT. *Powder Technology* **291**, 262–275.